ОПУБЛИКОВАННЫЕ СТАТЬИ В ПЕРЕВОДЕ НА АНГЛИЙСКИЙ ЯЗЫК

УДК 681.516.7
DOI: 10.22213/2413-1172-2022-3-100-107

Mathematical Model of Spatial Motion of the Controlled Parachute-Tether System of the Wind Kite Type*

V.M. Churkin, DSc (Physics and Mathematics), Moscow Aviation Institute (National Research University), Moscow, Russia
T.Y. Churkina, PhD in Engineering, Moscow Aviation Institute (National Research University), Moscow, Russia
A.M. Girin, PhD in Engineering, Moscow Aviation Institute (National Research University), Moscow, Russia

Mathematical modeling is created for the mathematical task of spatial motion of the controlled parachute-tether system of the "wind kite" type. The mathematical model parachute-tether system consists of a model of the main parachute and a model of the braking parachute. The parachutes are connected by the tether. The model of the main parachute is supposed to be the solid body. This solid body has two planes of symmetry. The braking parachute is the solid body with axial symmetry. The tether model is an absolutely flexible elastic thread. The tether is connected by ideal hinges with the main parachute and braking parachute.

The control of the main parachute is carried out by changing the length of the control slings. Changing the length causes deformation of the dome. This is the reason for the change in its aerodynamics. Maneuvering of the main parachute occurs in the vertical plane, when the length of the control slings changes simultaneously. Maneuvering of the main parachute in space is carried out when the length of the control slings changes, when the slings are given a travel difference.

The system of dynamic and kinematic equations is designed for calculating the controlled spatial movement of the main parachute, braking parachute and tether.

The option exists when the mass of the tether and the forces applied to the tether cannot be neglected. The motion of the tether is represented by the equations of motion of an absolutely flexible elastic thread in projections on the axis of a natural trihedron. The mathematical model is represented by a system of ordinary differential equations and partial differential equations. The problem is solved using various numerical methods. The solution is possible with the help of an integrated numerical and analytical approach as well.

Keywords: mathematical model, parachute-tether system, controlled parachute, dome aerodynamics, sling tension force.

Introduction

The actual problem today is the decanting of the payload with an accurate delivery to the required place on the earth's surface and the development of technical solutions for this [1]. This, for example, is associated with the fastest time to provide assistance to victims, the elimination of forest fires in hard-to-reach areas, as well as the risk of losing valuable amphibious equipment. The task of controlled descent of parachutes of various configurations was solved, for example, in [2-5]. Another relevant topic is the calculation of the parameters necessary for the soft landing of descent spacecraft (for example, Churkin V.M., Churkina T.Yu. "Mathematical model of the motion of a spacecraft with a combined soft landing system") or the launch of spacecraft into orbit using cable systems [6], as well as the removal of spacecraft that have spent their life from low orbits with landing at a safe point on the Earth's surface. One of the technically possible ways to solve such a problem can be the use of a parachute-tether system (PTS) of the "wind kite" type, consisting of a main parachute (MP) and a braking parachute (BP) connected to it by a tether.

The purpose of the study is to create a relatively simple mathematical model that allows determining the trajectory of the vehicle, and therefore the cargo.

* DOI: 10.22213/2413-1172-2021-4-17-24 (in Russ.).

Construction of a mathematical model of controlled spatial motion of the "wind kite" type PTS

There are various approaches to modeling and studying the movement of parachute systems or the movement of connected bodies [7-9]. The problem of mathematical modeling and investigation of the dynamics of the plane motion of a "wind kite" type PTS was solved in [10], on the basis of which we will construct a mathematical model of the spatial motion of such a PTS. Let's agree to consider the main parachute as a solid body having two planes of symmetry, its place of attachment of the parachute and tether ("koush") as an ideal hinge, the tether as an absolutely flexible weightless thread, and the braking parachute as an axisymmetric solid body. Let's assume that the main parachute's koush – the pressure center of the dome – and the center of mass lie on the intersection line of its symmetry planes. The center of pressure and the center of mass of the braking parachute lie at the same point located on the axis of symmetry of the parachute, the velocity of the incoming flow is a horizontal vector, the modulus of which depends only on the height H, and the changes atmospheric densities ρ of altitude H are extremely small. The MP is controlled by changing the length of the control lines, causing the dome to deformation and, as a consequence, changing its aerodynamics. With a simultaneous change in the length of the control lines by the amount of δ, the MP is maneuvered in a vertical plane, and when the length of the lines changes with a difference in stroke $\delta\Delta$, spatial maneuvering of the main parachute occurs. To simulate the spatial movement of the PTS (see Figure), the following coordinate systems are used: the $XOYZ$ absolute system; the $X_1O_1Y_1Z_1$ system connected to the MP; the $X_2O_2Y_2Z_2$ system connected to the tether (rope); the $X_3O_3Y_3Z_3$ system connected to the BP.

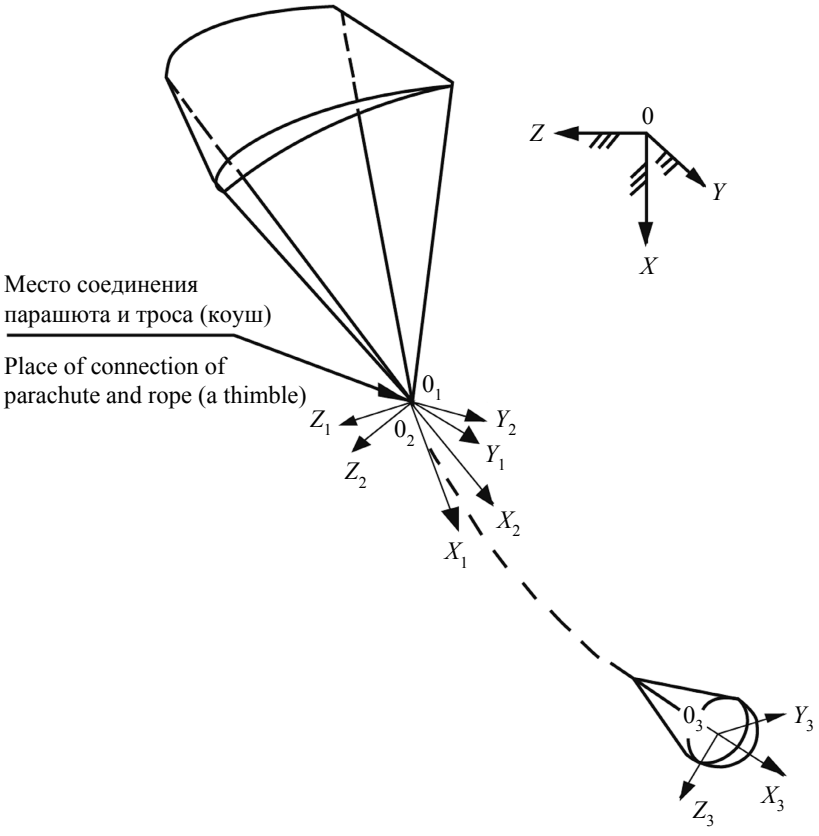

Parachute-rope system scheme of the type of a flying machine

The beginning of the $X_1O_1Y_1Z_1$ system is compatible with the main parachute's koush, and the O_1X_1 axis is directed along the line of intersection of the planes of symmetry. The beginning of the $X_2O_2Y_2Z_2$ system is also compatible with the main parachute's koush, and the O_2X_2 axis will be directed along the straight line connecting the O_2 point with the koush of the braking parachute. The beginning of the $X_3O_3Y_3Z_3$ system will be located in the center of mass of the braking parachute, and its axis of symmetry will be chosen as the O_3X_3 axis.

The dynamic equations of the MP in projections on the axis of the system $X_1O_1Y_1Z_1$ will be written as

$$\left(m+\lambda_{11}\right)\frac{dV_{ox}}{dt}+\lambda_{12}\left(\frac{dV_{oy}}{dt}-V_{ox}\omega_z\right)+$$
$$+\lambda_{16}\frac{d\omega_z}{dt}+\left(m+\lambda_{33}\right)V_{oz}\omega_y-\left(m+\lambda_{22}\right)\times$$
$$\times V_{oy}\omega_z+\left(\lambda_{11}-\lambda_{22}\right)W_o\omega_z\cos\theta_1+$$
$$+\lambda_{34}\omega_x\omega_y+\left(\lambda_{35}-ml_c\right)\omega_y^2-$$
$$-\left(\lambda_{26}-ml_c\right)\omega_z^2=-0,5\rho SV_D^2C_x+mg\times$$
$$\times\cos\theta_1\cos\gamma_1+R_{ox};$$

$$\left(m+\lambda_{22}\right)\frac{dV_{oy}}{dt}+\lambda_{12}\left(\frac{dV_{ox}}{dt}-V_{oy}\omega_z\right)+$$
$$+\left(\lambda_{26}+ml_c\right)\frac{d\omega_z}{dt}+\left(m+\lambda_{11}\right)V_{ox}\omega_z-$$
$$-\left(m+\lambda_{33}\right)V_{oz}\omega_x+\left(\lambda_{11}-\lambda_{22}\right)W_o\omega_z\sin\theta_1-$$
$$-\left(\lambda_{35}-ml_c\right)\omega_x\omega_y-\lambda_{34}\omega_x^2+\lambda_{16}\omega_z^2=$$
$$=-0,5\rho SV_D^2C_y+mg\sin\theta_1\cos\gamma_1+R_{oy};$$

$$\left(m+\lambda_{33}\right)\frac{dV_{oz}}{dt}+\lambda_{34}\frac{d\omega_x}{dt}+\left(\lambda_{35}-ml_c\right)\times \quad (1)$$
$$\times\frac{d\omega_y}{dt}-\left(m+\lambda_{11}\right)V_{ox}\omega_y+\left(m+\lambda_{22}\right)V_{oy}\times$$
$$\times\omega_x+\left(\lambda_{26}+ml_c\right)\omega_x\omega_z-$$
$$-\lambda_{12}\left(V_{oy}\omega_y-V_{ox}\omega_x\right)-\lambda_{16}\omega_y\omega_z=$$
$$=-0,5\rho SV_D^2C_z+mg\sin\gamma_1+R_{oz};$$

$$\left(J_x+\lambda_{44}\right)\frac{d\omega_x}{dt}-\left(J_{xy}-\lambda_{45}\right)\times$$
$$\times\left(\frac{d\omega_y}{dt}-\omega_x\omega_z\right)-\left(J_y-J_z+\lambda_{55}-\lambda_{66}\right)\omega_y\omega_z+$$
$$+\lambda_{16}V_{ox}\omega_y+\lambda_{34}\left(\frac{dV_{oz}}{dt}+V_{oy}\omega_x\right)+$$
$$+\left(\lambda_{26}+\lambda_{35}\right)\left(V_{oy}\omega_y-V_{oz}\omega_z\right)=0,5\rho SV_D^2m_x;$$

$$\left(J_y+\lambda_{55}\right)\frac{d\omega_y}{dt}-\left(J_{yx}-\lambda_{45}\right)\times$$
$$\times\left(\frac{d\omega_x}{dt}+\omega_y\omega_z\right)+\left(\lambda_{35}-ml_c\right)\left(\frac{dV_{oz}}{dt}-V_{ox}\omega_y\right)-$$
$$-\left(J_z-J_x+\lambda_{66}-\lambda_{44}\right)\omega_x\omega_z-\left(\lambda_{16}+\lambda_{34}\right)\times$$
$$\times\left(V_{ox}\omega_x-V_{oz}\omega_z\right)-\left(\lambda_{26}+ml_C\right)V_{oy}\omega_X=$$
$$=0,5\rho SV_D^2m_y-mgl_c\sin\gamma_1;$$

$$\left(J_z+\lambda_{66}\right)\frac{d\omega_z}{dt}+\lambda_{16}\left(\frac{dV_{ox}}{dt}-V_{oy}\omega_z\right)+$$
$$+\left(\lambda_{26}+ml_c\right)\left(\frac{dV_{oy}}{dt}+V_{ox}\omega_z\right)-$$
$$-\left(J_{zx}-\lambda_{35}\right)\left(\omega_x^2-\omega_y^2\right)-\left(J_x-J_y+\lambda_{55}-\lambda_{44}\right)\times$$
$$\times\omega_x\omega_y+\left(\lambda_{35}-ml_c\right)V_{oz}\omega_x-\lambda_{34}V_{oz}\omega_y=$$
$$=0,5\rho SV_D^2m_z-mgl_c\sin\theta_1\cos\gamma_1.$$

Here V_{ox},V_{oy},V_{oz} are the projections of the velocity vector of the main parachute koush; $\omega_x,\omega_y,\omega_z$ – projections of the vector of the angular velocity of rotation of the MP; V_D - the velocity of the pressure center of the MP dome relative to the incoming flow

$$V_D^2=\left(V_{ox}-W_0\sin\theta_1\cos\gamma_1\right)^2+$$
$$+\left(V_{oy}-W_0\cos\theta_1\cos\varphi_1-\omega_z l_D\right)^2+$$
$$+\left(V_{oz}+W_0\cos\gamma_1\cos\varphi_1+\omega_y l_D\right)^2,$$

where W_0 is the wind speed at the height H_0 of the main parachute's koush; m is the mass of the main parachute; $J_x,J_y,J_z,J_{xy},J_{yx},J_{zx}$ – axial and centrifugal moments of inertia of the main parachute relative to the axes of the associated coordinate system; $\lambda_{ij}\left(i,j=1,\ldots,6\right)$ – coefficients of the attached masses of the main parachute dome; R_{0x},R_{0y},R_{0z} – projections of the vector of the cable tension force in the main parachute's koush,

$$R_{0x}=R_0\left(a_{13}^1a_{13}^2+a_{23}^1a_{23}^2+a_{33}^1a_{33}^2\right);$$
$$R_{0y}=R_0\left(a_{12}^1a_{13}^2+a_{22}^1a_{23}^2+a_{32}^1a_{32}^2\right);$$
$$R_{0z}=R_0\left(a_{11}^1a_{13}^2+a_{21}^1a_{23}^2+a_{31}^1a_{33}^2\right);$$
$$a_{11}^j=\cos\gamma_j\cos\varphi_j;$$
$$a_{12}^j=\sin\theta_j\sin\gamma_j\cos\varphi_j-\cos\theta_j\sin\varphi_j;$$
$$a_{13}^j=\cos\theta_j\sin\gamma_j\cos\varphi_j+\sin\theta_j\sin\varphi_j;$$
$$a_{21}^j=\cos\gamma_j\sin\varphi_j;$$
$$a_{22}^j=\sin\theta_j\sin\gamma_j\sin\varphi_j+\cos\theta_j\cos\varphi_j;$$
$$a_{23}^j=\cos\theta_j\sin\gamma_j\sin\varphi_j-\sin\theta_j\cos\varphi_j;$$

$$a_{31}^{j} = -\sin\gamma_j; \quad a_{32}^{j} = \sin\theta_j \cos\gamma_j;$$

$$a_{33}^{j} = \cos\theta_j \cos\gamma_j,$$

where $\theta_j, \gamma_j, \varphi_j$ are the angles of rotation of the main parachute relative to the axes of the systems $X_1 O_1 Y_1 Z_1$ (when j = 1) and $X_2 O_2 Y_2 Z_2$ (when j = 2); $C_x, C_y, C_z, m_x, m_y, m_z$ – coefficients of aerodynamic forces and moments of the dome of the main parachute,

$$C_x = C_x(\alpha_1, \beta_1, \delta, \delta_\Delta); \quad C_y = C_y(\alpha_1, \beta_1, \delta, \delta_\Delta);$$

$$C_z = C_z(\alpha_1, \beta_1, \delta, \delta_\Delta); \quad m_x = m_x(\alpha_1, \beta_1, \delta, \delta_\Delta);$$

$$m_y = m_y(\alpha_1, \beta_1, \delta, \delta_\Delta); \quad m_z = m_z(\alpha_1, \beta_1, \delta, \delta_\Delta);$$

α_1, β_1 – angles of attack and sliding of the main parachute dome,

$$\alpha_1 = \operatorname{arctg}\left[\frac{\sqrt{\left(V_{oy} - W_0\cos\theta_1\cos\varphi_1 - \omega_z l_D\right)^2 + \left(V_{oz} + W_0\cos\gamma_1\cos\varphi_1 + \omega_y l_D\right)^2}}{V_{ox} - W_0\sin\theta_1\cos\gamma_1}\right];$$

$$\beta_1 = \operatorname{arctg}\left(\frac{V_{oz} + W_0\cos\gamma_1\cos\varphi_1 + \omega_y l_D}{V_{oy} - W_0\cos\theta_1\cos\varphi_1 - \omega_z l_D}\right),$$

where l_C, l_D are the distances from the koush to the center of mass and the center of pressure of the main parachute dome, respectively; S is the characteristic area of the main parachute dome; ρ is the air density.

When conducting trial calculations for modeling the spatial motion of a descending object with a controlled parachute, dependencies with the following structure were used for the coefficients C_x, C_y, C_z:

$$\begin{aligned} C_x &= C_{x0} + C_{x1}\alpha_1 + C_{x2}\alpha_1^2 + C_{x3}\alpha_1^3 + \\ &+ \left(C_{x01} + C_{x11}\alpha_1 + C_{x21}\alpha_1^2 + C_{x31}\alpha_1^3\right)\delta + \\ &+ \left(C_{x02} + C_{x12}\alpha_1 + C_{x22}\alpha_1^2 + C_{x32}\alpha_1^3\right)\delta^2 + \\ &+ \left(C_{x03} + C_{x13}\alpha_1 + C_{x23}\alpha_1^2 + C_{x33}\alpha_1^3\right)\delta^3 + C_{x4}\beta^2; \end{aligned}$$

$$\begin{aligned} C_y &= C_{y0} + C_{y1}\alpha_1 + C_{y2}\alpha_1^2 + C_{y3}\alpha_1^3 + C_{y4}\alpha_1^4 + \\ &+ \left(C_{y01} + C_{y11}\alpha_1 + C_{y21}\alpha_1^2 + C_{y31}\alpha_1^3 + C_{y41}\alpha_1^4\right)\delta + \\ &+ \left(C_{y02} + C_{y12}\alpha_1 + C_{y22}\alpha_1^2 + C_{y32}\alpha_1^3 + C_{y42}\alpha_1^4\right)\delta^2 + \\ &+ \left(C_{y03} + C_{y13}\alpha_1 + C_{y23}\alpha_1^2 + C_{y33}\alpha_1^3 + C_{y43}\alpha_1^4\right)\delta^3 + \\ &+ \left(C_{y04} + C_{y14}\alpha_1 + C_{y24}\alpha_1^2 + C_{y34}\alpha_1^3 + C_{y44}\alpha_1^4\right)\delta^4; \end{aligned}$$

$$C_z = \left(C_{z0} + C_{z1}\alpha_1\right)\left(\beta_1 + \delta_\Delta\right).$$

For a braking parachute, the dynamic equations in projections on the axis $X_3 O_3 Y_3 Z_3$ of the system are presented as follows:

$$\begin{aligned} &m_3\left(\frac{dV_{ox3}}{dt} + V_{oz3}\omega_{z3} - V_{oy3}\omega_{z3}\right) = \\ &= -0{,}5\rho S_3 V_{03}^2 \times C_{x3} + m_3 g\cos\theta_3\cos\gamma_3 + R_{Bx3}; \\ &m_3\left(\frac{dV_{oy3}}{dt} + V_{ox3}\omega_{z3} - V_{oz3}\omega_{x3}\right) = \\ &= -0{,}5\rho S_3 V_{03}^2 \times C_{y3} + m_3 g\sin\theta_3\cos\gamma_3 + R_{By3}; \\ &m_3\left(\frac{dVoz3}{dt} + V_{oy3}\omega_{x3} - V_{ox3}\omega_{y3}\right) = \\ &= -0{,}5\rho S_{03}^2 \times C_{z3} - m_3 g\sin\gamma_3 + R_{Bz3}; \\ &\frac{d\omega_{x3}}{dt} = 0; \\ &J_3\left(\frac{d\omega_{y3}}{dt} - \omega_{x3}\omega_{z3}\right) = 0{,}5\rho S_3 V_{03}^2 m_{y3} + l_3 R_{Bx3}; \\ &J_3\left(\frac{d\omega_{z3}}{dt} + \omega_{x3}\omega_{y3}\right) = 0{,}5\rho S_3 V_{03}^2 m_{z3} - l_3 R_{By3}. \end{aligned} \tag{2}$$

Here $V_{ox3}, V_{oy3}, V_{oz3}$ – projections of the velocity vector of the center of mass BP; $\omega_{x3}, \omega_{y3}, \omega_{z3}$ - projections of the angular velocity vector of rotation BP; V_{03} – velocity of the center of mass BP relative to the incoming flow,

$$\begin{aligned} V_{03}^2 &= \left(V_{ox3} - W_3\sin\theta_3\cos\gamma_3\right)^2 + \\ &+ \left(V_{oy3} - W_3\cos\theta_3\cos\varphi_3\right)^2 + \\ &+ \left(V_{oz3} + W_3\cos\gamma_3\cos\varphi_3\right)^2, \end{aligned}$$

where W_3 is the wind speed at the height H_3 of the center of mass of the BP; m_3 – the mass of the BP; J_3 – the moment of inertia of the BP relative to the axes $O_3 Y_3$ and $O_3 Z_3$; $R_{Bx3}, R_{By3}, R_{Bz3}$ – the projec-

tion of the vector of the tension force of the tether in the BP koush,

$$R_{Bx3} = R_B\left(a_{13}^3 a_{13}^2 + a_{23}^3 a_{23}^2 + a_{33}^2 a_{33}^2\right);$$

$$R_{By3} = R_B\left(a_{12}^3 a_{13}^2 + a_{22}^3 a_{23}^3 + a_{32}^3 a_{33}^2\right);$$

$$R_{Bz3} = R_B\left(a_{11}^3 a_{13}^2 + a_{21}^3 a_{23}^2 + a_{31}^3 a_{33}^2\right);$$

$\theta_3, \gamma_3, \varphi_3$ – the angles of rotation of the BP relative to the system; $C_{x3}, C_{y3}, C_{z3}, m_{y3}, m_{z3}$ – coefficients of the aerodynamic forces and moments of the BP,

$$C_{x3} = C_{x3}(\alpha_3);\ C_{y3} = C_{y3}(\alpha_3);\ C_{z3} = C_{z3}(\alpha_3);$$
$$m_{y3} = m_{y3}(\alpha_3);\ m_{z3} = m_{z3}(\alpha_3);$$

α_3 – angle of attack BP,

$$\alpha_3 = \operatorname{arctg}\left[\frac{\sqrt{\left(V_{oy3} - W_3\cos\theta_3\sin\varphi_3\right)^2 + \left(V_{oz3} + W_3\cos\gamma_3\cos\varphi_3\right)^2}}{V_{ox3} - W_3\sin\theta_3\cos\gamma_3}\right];$$

l_3 – the distance from the koush BP to its center of mass; S_3 – the characteristic area of the dome is BP.

The dynamic equations (1) and (2) are supplemented by the following kinematic equations:

$$\frac{d\theta_j}{dt} = \omega_{yj}\sin\theta_j\,\operatorname{tg}\gamma_j + \omega_{zj};$$

$$\frac{d\varphi_j}{dt} = \omega_{yj}\sin\theta_j\sec\gamma_j + \omega_{zj}; \qquad (3)$$

$$\frac{d\gamma_j}{dt} = \omega_{yj}\cos\theta_j, \quad j = 1, 2, 3.$$

$$\left(a_{11}^2\omega_{y2} - a_{12}^2\omega_{z2}\right)l_2 = a_{11}^3\left(V_{oz3} - \omega_{y3}l_3\right) + a_{12}^3\left(V_{oy3} + \omega_{z3}l_3\right) + a_{13}^3 V_{ox3} - a_{11}^1 V_{oz1} - a_{12}^1 \times V_{oy1} - a_{13}^1 V_{ox1};$$

$$\left(a_{21}^2\omega_{y2} - a_{22}^2\omega_{z2}\right)l_2 = a_{21}^3\left(V_{oz3} - \omega_{y3}l_3\right) + a_{22}^3\left(V_{oy3} + \omega_{z3}l_3\right) + a_{23}^2 V_{ox3} - a_{21}^1 V_{oz1} - a_{22}^1 \times V_{oy1} - a_{23}^1 V_{ox1}; \qquad (4)$$

$$\left(a_{31}^2\omega_{y2} - a_{32}^2\omega_{z2}\right)l_2 = a_{31}^3\left(V_{oz3} - \omega_{y3}l_3\right) + a_{32}^3\left(V_{jy3} + \omega_{z3}l_3\right) + a_{33}^3 V_{ox3} - a_{31}^1 V_{oz1} - a_{32}^1 \times V_{oy1} - a_{33}^1 V_{ox1};$$

$$\frac{dx}{dt} = V_{ox}a_{33}^1 + V_{oy}a_{32}^1 + V_{oz}a_{31}^1;$$

$$\frac{dy}{dt} = V_{ox}a_{23}^1 + V_{oy}a_{22}^1 + V_{oz}a_{21}^1; \qquad (5)$$

$$\frac{dz}{dt} = V_{ox}a_{13}^1 + V_{oy}a_{12}^1 + V_{oz}a_{11}^1,$$

where V_{ox}, V_{oy}, V_{oz}; $\omega_x, \omega_y, \omega_z$ – projections on the axis $X_2 O_2 Y_2 Z_2$ of the system of the koush velocity vector of the main parachute and the angular velocity vector of the rotation of the main parachute, respectively; l_2 - the distance between the couches of the main parachute and the braking parachute; x, y, z - the coordinates of the main parachute's koush in the system $XOYZ$.

In cases where the main and brake parachutes are connected by a long tether, the mass of which and the forces applied to it cannot be neglected, the equations of motion of the main and brake parachutes are supplemented by the equations of motion of the tether, as which the equations of motion of an absolutely flexible elastic thread, recorded in projections on the axis, can be used natural trihedron:

$$m_T\left(\frac{\partial V_\tau}{\partial t} - V_n\omega_b + V_b\omega_n\right) = \frac{\partial T}{\partial\sigma} + R_\tau;$$

$$m_T\left(\frac{\partial V_n}{\partial t} + V_\tau\omega_b - V_b\omega_\tau\right) = T\frac{\partial\varphi}{\partial\sigma} + R_n;$$

$$m_T\left(\frac{\partial V_b}{\partial t} + V_n\omega_\tau + V_\tau\omega_n\right) = R_b;$$

$$\frac{\partial V_\tau}{\partial\sigma} - V_n\frac{\partial\varphi}{\partial\sigma} = \frac{1}{f}\frac{\partial f}{\partial t};$$

$$\frac{\partial V_n}{\partial\sigma} + V_\tau\frac{\partial\varphi}{\partial\sigma} - V_b\frac{\partial\theta}{\partial\sigma} = \omega_b;$$

$$\frac{\partial V_b}{\partial\sigma} + V_n\frac{\partial\theta}{\partial\sigma} = -\omega_n; \qquad (6)$$

$$\frac{\partial\omega_\tau}{\partial\sigma} - \frac{\partial\Omega_\tau}{\partial t} = -\omega_n\Omega_b;$$

$$\frac{\partial\omega_n}{\partial\sigma} = \omega_\tau\Omega_b - \omega_b\Omega_\tau;$$

$$\frac{\partial\omega_b}{\partial\sigma} - \frac{\partial\Omega_b}{\partial t} = \omega_n\Omega_\tau;$$

$$\frac{\partial\theta}{\partial\sigma}=\Omega_{\tau};$$

$$\frac{\partial\varphi}{\partial\sigma}=\Omega_{b},$$

where V_{τ},V_{n},V_{b} – projections of the absolute velocity vector of the rope element; $\omega_{\tau},\omega_{n},\omega_{b}$ – projections of the absolute angular velocity vector of the rope element; Ω_{τ},Ω_{b} – projections of the Darboux vector; σ – the arc coordinate of the tether's element; φ, θ – the angles of curvature and torsion of the tether; T – the tension force of the tether; m_T – the linear density of the stretched tether; f – the coefficient of tension of the tether,

$$f=\frac{m_{T0}}{m_T},$$

where m_{T0} – linear density of an unstretched tether; R_{τ},R_{n},R_{b} – projections of the vector of the resultant of external forces applied to the tether.

If the stretching of the tether obeys Hooke's law, then

$$f=1+\alpha T,$$

where α – specific elongation of the tether,

$$\alpha=\frac{1}{E},$$

where E – modulus of elasticity of the tether.

The equations of the system (6) must be solved under boundary conditions, which are the equations of the system (1) at $\sigma=0$ $\left(V=V_0,T=R_0\right)$ and the equations of system (3) for $\sigma=l$ $\left(V=V_{03},T=R_B\right)$, where l – tether length.

Conclusions

1. A mathematical model of the spatial motion of the PTS is constructed taking into account the equations of motion of the tether in the form of systems of non-linear ordinary differential equations and partial differential equations.

2. The compilation of a system of dynamic and kinematic equations of spatial motion of a controlled PTS allows us to evaluate the main dynamic characteristics of the designed PTS and calculate their design parameters.

3. The obtained results can be used to determine the parameters of soft landing of descent spacecraft and aviation parachute systems, to calculate the operability of the elements of the PTS structure taking into account the dynamics of loading [11].

4. It should be noted that the greatest difficulties are caused by the study of the movement of the tether. A large number of publications by both domestic and foreign authors have been devoted to solving this problem. Moreover, such a task arises when studying the movement of the tether in various environments and not only for the PTS [12-16]. The calculation of tether systems is proposed for use during the descent of spent spacecraft and even in green energy systems [17-20], where various methods of numerical solution of the equations of tether movement are described. The analytical analysis of the dynamics of cable systems is based either on the linearization of the equations of motion of the cable, or on their extreme simplification and replacement by equations of model problems of mathematical physics. In a number of papers, it is proposed to use a complex numerical-analytical approach. The method of characteristics has become the most widespread, in which the analytical part of the study includes finding characteristics and recording the corresponding characteristic equations, and their integration is performed on a computer.

References

1. Jóźwiak A., Kurzawiński S. The Concept of Using the Joint Precision Airdrop System in the Process of Supply in Combat Actions. *Systemy Logistyczne Wojsk*, 2019, vol. 51, no. 2, pp. 27-42. DOI: 10.37055/slw/129219.

2. Fields T., Yakimenko O. Development of a Steerable Single-Actuator Cruciform Parachute. *J. of Aircraft*, 2018, vol. 55, no. 3, pp. 1041-1049. DOI: 10.2514/1.C034416.

3. Fields T., LaCombe J., Wang E. Time-Varying Descent Rate Control Strategy for Circular Parachutes. *J. of Guidance Control and Dynamics*, 2015, vol. 38, no. 8, pp. 1468-1477. DOI: 10.2514/1.G000627.

4. Gao X., Zhang O., Chen Q., Wang W. Fluid-structure Interactions on Steerable Cruciform Parachute Inflation Dynamics. 5th International Conference on Mechanical and Aeronautical Engineering (ICMAE 2019), Series: Materials Science and Engineering, 2019, vol. 751.

5. Fagley C., Seidel J., McLaughlin T., Noetscher G., Rose T. Computational Study of Air Drop Control Mechanisms for Cruciform Parachutes. AIAA 2017-3541, Session: Aerodynamic Decelerator Systems: Aerial Delivery, 2017. DOI: 10.2514/6.2017-3541.

6. Ledkov A. Modeling the spatial motion of a space tether system with an inflatable balloon for raising payload orbit. International Conference on Information Technology and Nanotechnology (ITNT), 2020, pp. 1-5. DOI: 10.1109/ITNT49337.2020.9253250.

7. Negrean I., Kacso K., Schonstein C., Duca A., Rusu F., Cristea F., Haragas S. New Formulations on Motion Equations in Analytical Dynamics. *Applied Me-*

chanics and Materials, 2016, vol. 823, pp. 49-54. DOI: 10.4028/www.scientific.net/AMM.823.49.

8. Roithmayr C., Beaty J., Pei J., Richard Barton R., Matz D. Linear Analysis of a Two-Parachute System Undergoing Pendulum Motion. AIAA 2019-3378, Session: Parachute Modeling and Analysis, 2019. Available at: https://doi.org/10.2514/6.2019-3378

9. Jing Pei J. Nonlinear Analysis of a Two-Parachute System Undergoing Pendulum Motion. AIAA 2019-3379, Session: Parachute Modeling and Analysis, 2019. Available at: https://doi.org/10.2514/6.2019-3379.

10. Churkin V.M. *Ustoychivost i kolebania parashutnih sistem* [Stability and vibrations parachute systems]. Moscow, URSS Publ., 2018, 230 p. (in Russ.)

11. Ivanov P. [Calculation of the Aerodynamic Load on the Gliding Parachute During Its Deployment and Overload Acting on the Dropped Object], *Vestnik Moskovskogo Aviatsionnogo Instituta = Aerospace MAI Journal*, 2021, vol. 28, no. 2, pp. 115-126. (in Russ.). DOI: 10.34759/vst-2021-2-115-126.

12. Li G., Shi G., Zhu Z.H. Three-Dimensional High-Fidelity Dynamic Modeling of Tether Transportation System with Multiple Climbers. *JGCD*, 2019, vol. 42, no. 8. DOI: 10.2514/1.G004118.

13. Htun T. Z., Suzuki H., Kuwano A., Tomobe H. Numerical Motion Analysis of ROV coupled with Tether Applying 24-DOFs Absolute Nodal Coordinate Formulation. Proc. of the Twenty-ninth International Ocean and Polar Engineering Conference, 2019, vol. 1, p. 1553. ISBN 978-1 880653 85-2; ISSN 1098-6189.

14. Suzuki H., Tomobe H., Kuwano A., Takasu K., Htun T.Z. Numerical Motion Analysis of ROV applying ANCF to Tether Cable Considering its Mechanical Property. Proc. of the Twenty-eight International Ocean and Polar Engineering Conference, 2018, vol. 1, pp. 365-372. ISBN 978-1-880653-87-6; ISSN 1098-6189.

15. Suzuki H., Yamazoe A., Htun T.Z. Numerical Modeling of Cable-winch System for ROV Launching and Recovering Processes based on the Finite Element Approach. Proc. of the Thirtieth International Ocean and Polar Engineering Conference, 2020, vol. 1, p. 1287. ISBN 978-1-880653-84-5; ISSN 1098-6189.

16. Liu C., Ding L., Gu J. Dynamic Modeling and Motion Stability Analysis of Tethered UAV. 5th International Conference on Robotics and Automation Sciences (ICRAS), 2021, pp. 106-110. DOI: 10.1109/ICRAS52289.2021.9476254.

17. Migliore H., McReynolds E. Ocean Cable Dynamics Using on Orthogonal Collocation Solution. *AIAA J.*, 1982, vol. 20, no. 8, pp. 1084-1091.

18. Razoumny Y., Kupreev S., Misra A.K. Method of Tethered System Control for Deorbiting Objects Using Earth's Atmosphere (IAA-AAS-DyCoSS3-152 – AAS 17-923), 2017. Available at: https://www.univelt.com/linkedfiles/v161%20Contents.pdf

19. Razoumny Y., Kupreev S., Misra A.K. The Research Method of Controlled Movement Dynamics of Tether System / Conference: First IAA/AAS SciTech Forum on Space Flight Mechanics and Space Structures and Materials. IAA-AAS-SciTech2018-113 – AAS 18-832, 2020, pp. 417-432. Available at: https://www.univelt.com/linkedfiles/v170%20Contents.pdf

20. Williams P., Lansdorp B., Ockels W. Optimal Crosswind Towing and Power Generation with Tethered Kites. *J. of Guidance, Control, and Dynamics*, 2009, vol. 31, no. 1, pp. 81-93. DOI: 10.2514/1.30089.

Математическая модель пространственного движения управляемой парашютно-тросовой системы типа «ветролет»

В. М. Чуркин, доктор физико-математических наук, Московский авиационный институт (Национальный исследовательский университет), Москва, Россия
Т. Ю. Чуркина, кандидат технических наук, Московский авиационный институт (Национальный исследовательский университет), Москва, Россия
А. М. Гирин, кандидат технических наук, Московский авиационный институт (Национальный исследовательский университет), Москва, Россия

Представлено математическое моделирование пространственного движения управляемой парашютно-тросовой системы типа «ветролет». Рассматриваемая система представляется моделью, составленной из основного парашюта и тормозного парашюта, соединенных тросом. Основной парашют считается твердым телом, имеющим две плоскости симметрии, а тормозной парашют – осесимметричным твердым телом. Трос рассматривается как абсолютно гибкая упругая нить, соединенная идеальными шарнирами с основным и тормозным парашютами. Управление основным парашютом осуществляется путем изменения длины управляющих строп, вызывающего деформацию купола и, как следствие, изменение его аэродинамики. При одновременном изменении длины управляющих строп происходит маневрирование основного парашюта в вертикальной плоскости, а при изменении длины управляющих строп с заданной разностью хода – пространственное маневрирование основного парашюта. Составлена система динамических и кинематических уравнений пространственного движения основного парашюта, тормозного парашюта и троса. В случаях, когда основной и тормозной парашюты соединены тросом, массой которого и приложенными к нему силами пренебречь нельзя, его движение представляется уравнениями движения абсолютно гибкой упругой нити в проекциях на оси естественного трехгранника. В результате предлагаемая математическая модель представляется системой обыкновенных дифференциальных уравнений и дифференциальных уравнений в частных производных, для решения которых могут быть использованы различные численные методы или комплексный численно-аналитический подход. Например, при решении методом характеристик аналитическая часть ис-

следования включает нахождение характеристик и запись соответствующих характеристических уравнений с последующим их численным интегрированием.

Ключевые слова: математическая модель, парашютно-тросовая система, управляемый парашют, аэродинамика купола, сила натяжения троса.

Получено 07.06.2021

For Citation

Churkin V.M., Churkina T.Y., Girin A.M. Mathematical Model of Spatial Motion of the Controlled Parachute-Tether System of the Wind Kite Type = Matematicheskaya model' prostranstvennogo dvizheniya upravlyaemoi parashyutno-trosovoi sistemy tipa "vetrolet". *Vestnik IzhGTU imeni M.T. Kalashnikova*, 2022, vol. 25, no. 3, pp. 100-107. DOI: 110.22213/2413-1172-2022-3-100-107. DOI: 10.22213/2413-1172-2021-4-17-24 (in Russ.).